SELF-MAGNETICALLY INSULATED TRANSMISSION LINE (MITL) SYSTEM DESIGN FOR THE 20-STAGE HERMES-III ACCELERATOR*

R. C. Pate, J. C. Patterson, M. C. Dowdican, J. J. Ramirez,
D. E. Hasti, K. M. Tolk, J. W. Poukey, L. X. Schneider,
S. E. Rosenthal, T. W. L. Sanford, J. A. Alexander, C. E. Heath
Sandia National Laboratories
Albuquerque, New Mexico 87185

ABSTRACT

The Hermes-III MITL is a coaxial waveguide structure that is divided into two functional regions: 1) a 12.8-m long "voltage adder" section, and 2) a 4.6-m long "isolator/extension" section. The adder MITL provides the means for the series "addition" of the input voltages from the individual cavity feeds. The isolator/extension MITL provides efficient power transport and isolation from the output of the adder section to a bremsstrahlung diode. This paper describes the Hermes-III MITL and presents the electrical design methodology, models, and results obtained for optimum system operation.

INTRODUCTION

Hermes III is a relativistic electron beam accelerator designed to deliver a nominal 20-MV, 800-kA, power pulse to a bremsstrahlung diode. The purpose of the system is to provide a uniform source of intense gamma radiation over a large cylindrical volume for use in weapons effects simulation tests[1].

The accelerator design is based on a cavity-fed, self-magnetically insulated transmission line (MITL) system which performs the series addition of voltage pulses from multiple source modules. The sources consist of 20 identical, inductively-isolated, cavity feed systems[2]. The concept of a cavity-fed MITL voltage adder has been successfully demonstrated with the 4-MV, 4-cavity HELIA accelerator[3].

Each cavity is a toroidal structure that is driven simultaneously by four 5-Ω pulse-forming lines (PFLs). The PFL outputs are mixed in parallel and delivered with azimuthal symmetry to a 3.8-cm circumferential feed gap in the inside surface of the cavity bore. The cavities contain magnetic cores[4] that provide inductive isolation necessary for voltage addition during pulsed operation.

The coaxial MITL system consists of two distinct regions as shown in Fig. 1. The first is the 12.8-m "adder" section that extends through the center bore formed by the longitudinal assembly of 20 cavity toroids. The second region is the 4.6-m "isolator/extension" section that connects the adder output to the electron beam diode. The extension serves as a matched load impedance for the adder and provides efficient power transport to the diode. It also provides time isolation which makes operation of the adder largely independent of diode impedance conditions. Not shown in the extension section in Fig. 1 is a constant impedance biconic taper that reduces the MITL dimensions down to two different diode sizes. The two diodes have cathode radii of 18.5-cm and 12-cm, respectively[5]. Electron loss from this taper region has been investigated through computer simulations using a self-consistent, 2-D electromagnetic particle-in-cell (PIC) code[6]. The simulations were done on a 3-m extension MITL with a matched diode termination. Simulation results for an abrupt step transition in both anode and cathode showed an 11% current loss. Replacing the abrupt steps with gradual tapers resulted in no current loss. This result indicates that biconic taper angles within about 3° are sufficiently gentle to keep losses to a negligible level.

*This work was supported by the U.S. Department of Energy under Contract DE-AC04-76DP00789.

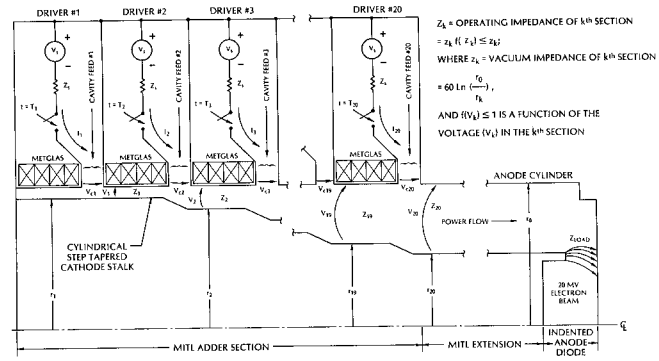

Figure 1. Schematic cross section of the Hermes III adder/extension MITL system.

The outer conductor (anode) of the adder MITL is formed by the inner surface of the cavities, and has an inside radius of 38.1-cm. This surface is interrupted at regular intervals by the cavity feed gaps. The inner conductor of the adder is formed by a cantilevered cathode stalk that is centered and aligned[7] within the anode cylinder. Proper MITL alignment is necessary to maintain azimuthally symmetric power flow. Tests were conducted on HELIA to help establish alignment criteria. The tests involved observing the operational impact of relative tilt and offset between the MITL anode and cathode surfaces. Test results indicate that misalignment within 5% of the local radial gap can be tolerated with negligible effect on power flow symmetry and efficiency.

The cathode stalk decreases in radius toward the downstream (high voltage output) end of the adder. The transitions in radius take the form of short (~3.8-cm) tapered steps that are longitudinally aligned with the adjacent anode feed gaps. This geometry is a departure from the continuously tapered cathode stalk first used in the 4-cavity HELIA adder[3]. The continuous taper was used largely out of concern over possible electron loss from relatively abrupt transitions in cathode radius. PIC code simulations of an adder MITL with discrete cathode steps, and recent HELIA tests using adder cathodes with linearly tapered steps show no step-induced current losses.

The cathode geometry in Fig. 1 is preferred over a continuous taper for several reasons. As shown in the figure, the cathode has constant radius between cavity feeds. This is easier and cheaper to manufacture than a continuous taper, especially when tight mechanical tolerances are required. The constant radius cathode segments provide constant vacuum impedance along each MITL segment, with the impedance "profile" increasing in a step-wise fashion at each successive cavity feed location. The vacuum impedance profile is related to the coaxial MITL dimensions of Fig. 1 by

$$z_k = 60 \ln(r_0/r_k)\ [\Omega]\ ; \quad k=1,2,\ldots,20. \qquad (1)$$

where r_0=38.1-cm is the fixed anode radius, and r_k is the cathode radius of the k-th MITL segment. In the

Report Documentation Page

Form Approved
OMB No. 0704-0188

1. REPORT DATE	2. REPORT TYPE	3. DATES COVERED
JUN 1987	**N/A**	**-**

4. TITLE AND SUBTITLE	5a. CONTRACT NUMBER
Self-Magnetically Insulated Transmission Line (Mitl) System Design For The 20-Stage Hermes-Iii Accelerator	5b. GRANT NUMBER
	5c. PROGRAM ELEMENT NUMBER
6. AUTHOR(S)	5d. PROJECT NUMBER
	5e. TASK NUMBER
	5f. WORK UNIT NUMBER
7. PERFORMING ORGANIZATION NAME(S) AND ADDRESS(ES) **Sandia National Laboratories Albuquerque, NM 87185**	8. PERFORMING ORGANIZATION REPORT NUMBER
9. SPONSORING/MONITORING AGENCY NAME(S) AND ADDRESS(ES)	10. SPONSOR/MONITOR'S ACRONYM(S)
	11. SPONSOR/MONITOR'S REPORT NUMBER(S)

12. DISTRIBUTION/AVAILABILITY STATEMENT
Approved for public release, distribution unlimited

13. SUPPLEMENTARY NOTES
See also ADM002371. 2013 IEEE Pulsed Power Conference, Digest of Technical Papers 1976-2013, and Abstracts of the 2013 IEEE International Conference on Plasma Science. Held in San Francisco, CA on 16-21 June 2013. U.S. Government or Federal Purpose Rights License

14. ABSTRACT
The Hermes-III MITL is a coaxial waveguide structure that is divided into two functional regions: 1) a 12.8-m long "voltage adder" section, and 2) a 4.6-m long "isolator/extension" section. The adder MITL provides the means for the series "addition" of the input voltages from the individual cavity feeds. The isolator/extension MITL provides efficient power transport and isolation from the output of the adder section to a bremsstrahlung diode. This paper describes the Hermes-III MITL and presents the electrical design methodology, models, and results obtained for optimum system operation.

15. SUBJECT TERMS

16. SECURITY CLASSIFICATION OF:			17. LIMITATION OF ABSTRACT	18. NUMBER OF PAGES	19a. NAME OF RESPONSIBLE PERSON
a. REPORT	b. ABSTRACT	c. THIS PAGE			
unclassified	**unclassified**	**unclassified**	**SAR**	**4**	

presence of trapped electron flow, the actual operating impedance of each MITL segment depends on the segment voltage, and will be somewhat less than the local vacuum impedance. When properly designed and operated, the individual MITL segments in the adder system will each function in the self-limited mode in such a way that each cavity driver will experience the same effective load impedance. Assuming equal source voltages, each cavity feed will then deliver equal voltage and current (power flow) to the MITL system. This is called "balanced" system operation, and it requires that each MITL segment operate with a constant impedance over its length. This is best achieved by the piece-wise constant radius cathode stalk geometry of Fig. 1.

The MITL system design process essentially reduces to choosing the required cathode stalk dimensions to give the proper impedance profile for balanced power flow at some optimum accelerator operating point. The remainder of this paper discusses the design and operation of an optimum MITL system for Hermes III.

POWER FLOW SYSTEM MODELING AND CONSTRAINTS

The overall power flow system shown in Fig. 1 can be represented by the generalized network model shown in Fig. 2. In this model, the 20 identical source terms each consist of an ideal 1.25-Ω PFL voltage source followed by a block representing the cavity system. The PFL voltage source is a symmetrical trapezoid with a peak open-circuit amplitude (V_{pfl}) that is nominally 2-MV. The output of this source model into a 1.5-Ω resistive load is a pulse with 17-ns risetime (10-90%) and 40-ns width (FWHM). These characteristics are representative of actual PFL/cavity output measurements, including the effects of switch jitter[2]. To be within safe operating limits, the PFL open-circuit voltage should not exceed ~2.2-MV.

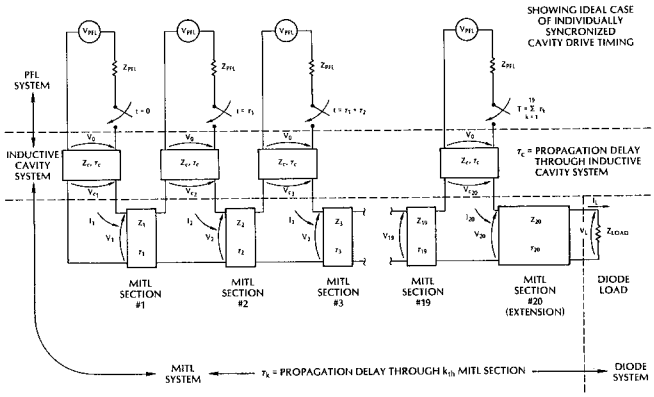

Figure 2. Block diagram of a generalized 20-stage PFL/CAVITY/MITL/LOAD network model.

Several multi-element equivalent circuit models have been developed[2,8] that closely describe the dynamic behavior of the cavity system. Cavity model calculations using the SNLA circuit simulation code SCREAMER[9] show that the entire PFL/cavity network can be approximated by a Thevenin equivalent source with an open circuit voltage of $2V_0 = 1.32(V_{pfl})$ and an impedance of $Z_c = \sim 2.4\text{-}\Omega$. The load voltage V_1, corresponding to the cavity feed gap output voltage across load Z_1, is then given by

$$V_1 = 2\,V_0 Z_1/(Z_1 + Z_c) = 1.32\,V_{pfl} Z_1/(Z_1 + 2.4). \quad (2)$$

To be within safe operating limits, the cavity feed gap voltage should not exceed ~1.1-MV.

The ideal timing shown in Fig. 2 is such that downstream sources are sequentially switched in sync with the wavefront propagating in the adder MITL. The source switching in Hermes III is actually done in 5 groups of 4 cavities each[1]. Although group timing does not allow for exact gap-to-gap pulse synchronization, the worst case timing errors between adjacent gaps will be no more than about 2-ns. Such errors will cause some degradation at edges, but will not effect the middle, steady-state region of the pulse. Because the design approach presented here is based on steady-state flow theory arguments, the assumption of ideal timing will not alter the design results.

An important design goal for the adder section is balanced (equal) power flow from the 20 individual sources. As previously discussed, this demands that the MITL system behave in such a way that each source sees the same effective load impedance during the time of its pulse delivery. Because each source is assumed to have the same voltage and output impedance, this balanced operation will be achieved by demanding equal steady-state pulse current for each segment

$$I_1 = I_2 = \ldots = I_{20} = I. \quad (3)$$

Each segment will initially operate self-limited with an input current flow and impedance that are appropriate for the local segment input voltage. With ideal source timing (neglecting finite risetime effects) and the demand that current flow be uniform according to Eq. (3), the mesh equations of the model in Fig. 2 (with the network sources replaced by the simpler equivalent sources) demand that the MITL segments satisfy the operating impedance relationship given by

$$Z_k = k\,Z_1 \quad ; \quad k = 1,2,\ldots,20\,, \quad (4)$$

where Z_k is the steady-state operating impedance of the k-th segment, and Z_1 is the effective load impedance that will be seen by each cavity. Z_{20} is the effective input impedance of the isolator/extension MITL section. With synchronized source timing, each MITL segment will see a "matched" termination presented by the next (downstream) source/MITL segment combination. This dynamic impedance match condition occurs only during synchronized driver operation. The resulting MITL segment operating voltages will then be given by

$$V_k = k\,V_1 \quad ; \quad k = 1,2,\ldots,20\,, \quad (5)$$

where V_1 is the output voltage developed across each cavity feed gap. The system current (I), the PFL source voltage (V_{pfl}), and the effective cavity load impedance (Z_1) are approximately related by

$$I = 2V_0/(Z_c + Z_1) = 1.32(V_{pfl})/(2.4 + Z_1), \quad (6)$$

and the output cavity feed voltage is given approximately by

$$V_1 = I\,Z_1 = 1.32\,Z_1 V_{pfl}/(2.4 + Z_1). \quad (7)$$

If the assumptions and relationships in the above analysis are satisfied, the adder MITL will operate in a unified fashion that can be viewed as a single source/MITL element driving the matched extension MITL with an output impedance of $Z_{20} = 20(Z_1)$, an output voltage of $V_{20} = 20(V_1)$, and a self-limited current flow of I. Adder operation is independent of diode impedance conditions during most of the pulse due to the time isolation afforded by the extension MITL.

OPTIMUM SYSTEM OPERATING POINT

The radiation output from the Hermes-III bremsstahlung diode[5] is expected to scale according to a power law of the form[10]

$$\text{Dose Rate} \;\alpha\; Q = I_d(V_d)^{2.2}, \qquad (8)$$

where I_d and V_d are the diode current and voltage, and Q is a "quality factor" proportional to the dose rate downstream of the diode. This scaling law assumes a time-invariant electron flow pattern over the pulse duration. The Q factor is used as an indicator of expected radiation output, where the diode is approximated by a resistive load. For maximum efficiency, the diode is assumed matched to the MITL system self-limited output impedance. The relationships given by equations (4)-(8) provide a means of describing the operating point of the "balanced" power flow system as a function of the source parameters, MITL parameters, and the radiation output parameter.

Figure 3 shows a family of curves which relate the normalized diode radiation output, MITL system output impedance, and PFL charge voltage. The quality factor (Q) has been normalized to the value (Q_0) for the nominal V_d, I_d conditions of 20-MV, 800-kA. The nominal Hermes-III radiation output goals can be met by a 20-MV, 500-kA electron beam delivered to the diode target with no losses and normal beam incidence. These conditions yield a minimum Q/Q_0 value of 0.625, which is also shown in Fig. 3.

Two cavity feed voltage contours are also shown in Fig. 3. The safe operating region for the system is the area below the V_{pfl}= 2.2-MV contour and the 1.1-MV cavity feed voltage contour. Within this allowed operating region, the peak diode output is 15% above the nominal output specification and occurs when V_{pfl} is at the limiting value of 2.2-MV and the MITL output impedance is about 30-Ω. This corresponds to Z_1= 1.5-Ω. Using these values in Eq. (5) - Eq. (7) gives an adder system output of approximately 22.3-MV at 741-kA. This operating point is taken to be optimum on the basis of maximizing the diode radiation output within the safe operating limits of the accelerator.

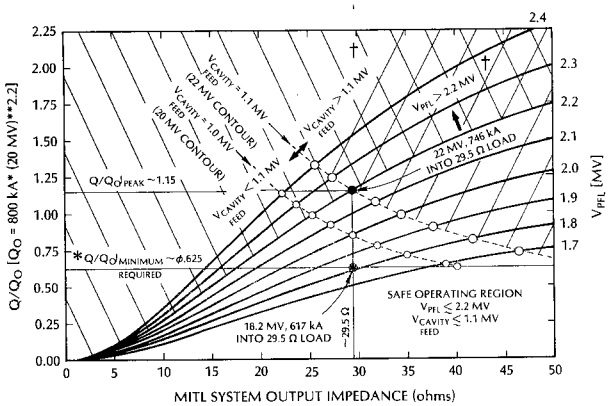

* BASED ON A MINIMUM REQUIRED Q OF (20 MV)$^{2.2}$ (500 kA) AT THE DIODE CONVERTER WITH NO LOSSES

† SHADED AREAS (CROSS-HATCHED) ARE OUTSIDE OF THE SAFE OPERATING REGION

Figure 3. Operating point parameter plot for Hermes III with a balanced MITL design and a matched load impedance. Parameter Q is a measure of peak diode output radiation dose rate, with Q_0 being the nominal value at 20-MV, 800-kA.

SELF-LIMITED MINIMUM CURRENT MITL DESIGN

The self-limited operating point of each of the MITL segments corresponds closely with the minimum current point as calculated from Creedon's Brillouin flow model[11]. Minimum current solutions from Creedon's model agree with the planar[12] and coaxial[13] pressure balance models to within 2% and 1%, respectively. The Creedon model results also agree with PIC code simulations to within 10%[5,6,14].

From Creedon's model we have

$$z_k = (511/I)\;\gamma_{sk}^{3}\;\ln(\gamma_{sk}+(\gamma_{sk}^{2}-1)^{1/2}), \qquad (9)$$

where z_k is the vacuum impedance of k-th segment (Ω), I is the minimum steady-state current flow (kA), and γ_{sk} is the relativistic factor for electrons at the boundary of the electron sheath in the k-th segment. Parameter γ_{sk} is found by solving the equation

$$V_k/511 = \gamma_{sk}+(\gamma_{sk}^{2}-1)^{3/2}\ln(\gamma_{sk}+(\gamma_{sk}^{2}-1)^{1/2})-1, \qquad (10)$$

where V_k is the k-th segment operating voltage (kV). MITL system radii are found by applying the relationship of equation (1) to the results of equation (9). The minimum current 30-Ω MITL design for the optimum Hermes-III system operating point is given in Table 1.

Table 1. HERMES III SELF-LIMITED MINIMUM CURRENT MITL DESIGN FOR OPTIMUM 30-Ω SYSTEM OPERATING POINT

V_{pfl}= 2.2-MV, I = 741-kA

ANODE RADIUS (r_0) = 38.1-cm

MITL SEGMENT k	SEGMENT VOLTAGE V_k[MV]	CATHODE RADIUS r_k[cm]	SHEATH FACTOR γ_{sk}	VACUUM IMPEDANCE z_k[Ω]	OPERATING IMPEDANCE Z_k[Ω]
1	1.11	36.54	1.55	2.51	1.50
2	2.22	35.39	1.76	4.42	3.00
3	3.34	34.36	1.92	6.21	4.50
4	4.45	33.38	2.05	7.94	6.00
5	5.56	32.45	2.16	9.63	7.50
6	6.68	31.55	2.25	11.31	9.00
7	7.79	30.69	2.34	12.98	10.50
8	8.90	29.86	2.41	14.63	12.00
9	10.01	29.05	2.48	16.27	13.50
10	11.13	28.27	2.55	17.90	15.00
11	12.24	27.51	2.61	19.53	16.50
12	13.35	26.78	2.67	21.15	18.00
13	14.46	26.07	2.72	22.77	19.50
14	15.58	25.38	2.77	24.38	21.00
15	16.69	24.71	2.82	25.99	22.50
16	17.80	24.06	2.87	27.59	24.00
17	18.92	23.42	2.91	29.19	25.50
18	20.03	22.81	2.95	30.79	27.00
19	21.14	22.21	2.99	32.38	28.50
20	22.25	21.63	3.03	33.98	30.00

SIMULATION RESULTS

Computer simulation of the Hermes-III MITL system has been done with both a 2-D PIC code[6] and with the SCREAMER network code[9] incorporating a lossy MITL model similar to that developed by Bergeron[15]. The lossy MITL network model uses a voltage-dependent impedance function based on the Creedon minimum current model.

Figure 4 shows network simulation results for the circuit model shown in Fig. 2 using the optimum 30-Ω MITL design operating at V_{pfl}=2.2-MV with a matched resistive load. Shown plotted are voltages at the diode load for four different cases: a) lossless transmission line (TL) model with ideal individual source timing; b) lossless TL model with group timing; c) lossy MITL model with ideal timing; and d) lossy MITL model with group timing. The "ideal" timing referred to above means close synchronization of each individual driving source with the wavefront within the MITL system. This is in contrast to the group timing actually used in Hermes III. The comparison plots demonstate that, in terms of peak pulse

amplitude, the behavior of the more elaborate system model is in basic agreement with the approximate network analysis used to arrive at the optimum MITL design. Departure from an ideal trapezoidal pulse shape is due mainly to the dynamic characteristics of the combined PFL/cavity system source. Comparison of a) and c) with b) and d) show that lack of individual cavity timing causes only slight degradation in the output pulse. The lossy MITL model primarily introduces pulse sharpening through edge errosion effects, as can be seen by comparing curves c) and d) with a) and b). Curve d) is representative of the expected output of the 30-Ω MITL design at the optimum system operating point. The pulse has a rise time (10-90%) of 13-ns and a width (FWHM) of 33-ns with a peak of 22.5-MV. The peak output current flow of ~750-kA is uniform within 5% throughout the MITL system. The peak cavity feed voltage is ~1.13-MV. Variations in adder segment current and cavity feed voltage are primarily due to the effects of group timing. Simulations also show that the system will deliver 20-MV, 800-kA to an undermatched ~25-Ω diode with little impact on the operating point of the adder section.

A PIC code simulation[6] was done on a portion of this system consisting of the last cavity feed in the adder section and the first 2-m of extension MITL. The simulation resulted in self-limited operation at 22.4-MV and 780-kA (divided between 300-kA boundary, 480-kA electron sheath). The operating impedance of 28.7-Ω predicted by the PIC calculations is within 5% of the 30-Ω minimum current design.

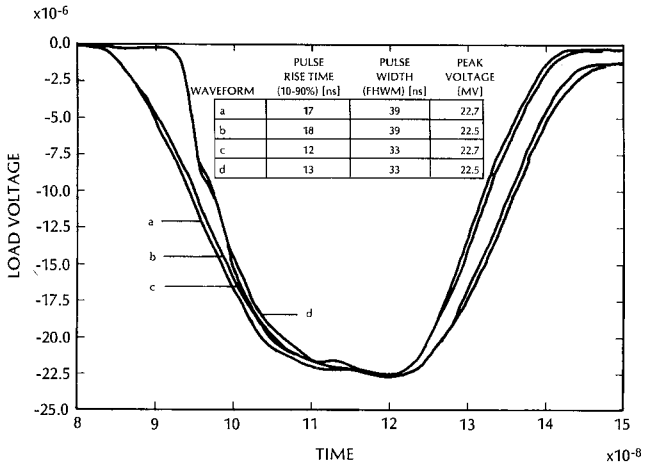

WAVEFORM	PULSE RISE TIME (10-90%) [ns]	PULSE WIDTH (FHWM) [ns]	PEAK VOLTAGE [MV]
a	17	39	22.7
b	18	39	22.5
c	12	33	22.7
d	13	33	22.5

Figure 4. Network simulation results for the optimum Hermes III system operating at V_{pfl}= 2.2-MV with a 30-Ω MITL output impedance and a matched resistive load. The plots are of load voltage for 4 cases: a) lossless transmission line (TL) system w/ ideal cavity timing; b) lossless TL system w/ group timing; c) lossy MITL system w/ ideal timing; d) lossy MITL system w/ group timing.

CONCLUSIONS

A procedure for designing the 20-stage Hermes-III MITL system has been presented. The design equalizes power flow from each of the 20 cavity sources and assumes self-limited MITL operation at minimum current as calculated with Creedon's parapotential flow model. The resulting adder section functions as a unified, self-limited MITL driver whose operation is largely independent of diode load conditions due to time isolation. Both PIC code and network code simulation results agree closely with the approximate design predictions.

A 30-Ω output impedance MITL design combined with pulsed-power system operation at an open-circuit PFL charge voltage of 2.2-MV appears to be optimum for peak radiation production within the safe operating limits of the accelerator. This will provide an output of about 22.5-MV at 750-kA into a matched 30-Ω diode, giving a possible 15% dose rate improvement over the nominal 20-MV, 800-kA specification.

Adder output pulse degradation due to lack of individual cavity timing does not appear to be a severe problem. Pulse sharpening through edge erosion processes in the MITL is expected to shorten the rise time and width of the pulse actually delivered to the diode, allowing for possible further improvement in the radiation pulse. Should additional pulse sharpening prove necessary, provision is being made for inclusion of a plasma opening switch (POS) system in the extension MITL just upstream of the diode. The inclusion of a constant impedance biconic taper region in the extension MITL will give the flexibility of using two different sizes of diode, allowing for tradeoffs between radiation field intensity and uniformity[5].

REFERENCES

1. J. J. Ramirez et al.,"The Hermes III Program", in these proceedings.
2. D. L. Johnson et al., "Hermes-III Cavity Prototype Tests", in these proceedings.
3. J. J. Ramirez et al., Proc. 5th Int'l. IEEE Pulsed Power Conf., Arlington, VA, p.143 (June 10-12, 1985).
4. C. W. Huddle et al., "Testing of the Inductive Cores for Hermes III", in these proceedings.
5. T. W. L. Sanford et al., "Indented-Anode Diode for Hermes III", in these proceedings.
6. J. W. Poukey, Report SAND87-0531, Sandia National Laboratories, Albuquerque, NM (April, 1987).
7. E. L. Burgess et al., "Alignment of the Hermes III Magnetically Insulated Transmission Line", in these proceedings.
8. L. Schlitt, W. Weseloh, I. Smith, V. Bailey, D. Garofalo, and D. Battilana, Report PSI-FR-234-3, Pulse Sciences, Inc., May 1986.
9. M. M. Widner and M. L. Kiefer, "SCREAMER User's Guide", Sandia National Laboratories, Albuquerque, NM, (April, 1985).
10. T. W. L. Sanford et al., "Dose-Voltage Dependence for the HELIA/Hermes-III Bremsstrahlung Diodes", Paper H10, 1987 Part. Accel. Conf., Wash. D.C. (March, 1987).
11. J. M. Creedon, J. Appl. Phys., V.48, No.3, pp. 1070-1077, (1977).
12. C. W. Mendel, Jr., D. B. Seidel, and S. E. Rosenthal, Laser and Part. Beams, V.1, part 3,. pp. 311-320, (1983).
13. S. E. Rosenthal and C. W. Mendel, Jr., PBF Prog. Report: July-Dec., 1985, Sandia National Labs, Albuquerque, NM (1986).
14. J. W. Poukey and K. D. Bergeron, Appl. Phys. Lett., V. 32, No. 1, pp. 8-10, (1978).
15. K. D. Bergeron, J. Appl. Phys., V. 48, No. 7, pp. 3065-3069, (1977).